Microscopic analysis for water stressed by high electric fields in the prebreakdown regime

R. P. Joshi, J. Qian, and K. H. Schoenbach
Department of Electrical and Computer Engineering, Old Dominion University, Norfolk, Virginia 23529-0246

E. Schamiloglu
Department of Electrical and Computer Engineering, University of New Mexico, Albuquerque, New Mexico 87131

(Received 16 January 2004; accepted 11 July 2004)

Analysis of the electrical double layer at the electrode-water interface for voltages close to the breakdown point has been carried out based on a static, Monte Carlo approach. It is shown that strong dipole realignment, ion-ion correlation, and finite-size effects can greatly modify the electric fields and local permittivity (hence, leading to optical structure) at the electrode interface. Dramatic enhancements of Schottky injection, providing a source for electronic controlled breakdown, are possible. It is also shown that large pressures associated with the Maxwell stress tensor would be created at the electrode boundaries. Our results depend on the ionic density, and are in keeping with recent observations. A simple, perturbative analysis shows that high field regions with a sharp variation in permittivity can potentially be critical spots for instability initiation. This suggests that the use of polished electrodes, or composite materials, or alternative nonpolar liquids might help enhance high-voltage operation. © *2004 American Institute of Physics*. [DOI: 10.1063/1.1789274]

I. INTRODUCTION

There is considerable interest in the study of electrical breakdown in water (and other liquids) for a variety of reasons.[1] Practical applications of dielectric liquids include water-filled gaps for the design of acoustic equipment,[2,3] the insulation of high-voltage devices,[4] as the medium in spark erosion machines,[5] and use in energy storage and switching elements for pulsed power systems. Generally, for high-voltage pulsed power systems, solids or gases at high pressure have been used as the dielectric material. However, the use of polar liquids seems to have advantages for energy storage and as switch media, particularly for nanosecond pulse generators. Polar liquids not only have a high dielectric constant but also have a higher breakdown strength than compressed gases.[6] Water, for example, has been used and found to hold off electrical fields up to 1 MV/cm for durations up to hundreds of nanoseconds.[7] In comparison to solids, their ability to circulate leads to better thermal management and easier removal of debris after breakdown. Liquid dielectrics are also better suited for applications involving complex geometries.

Though electrical behavior of dielectric liquids (especially water) subjected to high electric fields has been intensively studied,[8–17] there is still no comprehensive understanding of all the inherent physics. Part of the problem is that liquids lack the long-range order and periodicity that is inherent in solids. This makes it difficult to obtain exact repeatable results since the electrical behavior is inherently stochastic in nature. Examples include random treeing patterns[18–22] and surface discharges with Lichtenberg figures.[18,22] Another complication is that conduction is strongly influenced by both the liquid-electrode interface and bulk properties that include a variety of electric-field and temperature-dependent processes.[23–25] The role of heating and discharges within the thermally generated vapor bubbles have been advanced as potential mechanisms, since electron avalanche processes in liquids (e.g., water) are known to be negligible.[26] However, such internal heating can only be possible if the duration of the applied voltage is sufficiently long, i.e., at least in 10–100 μs range or larger. In recent experiments, however, breakdown of water filled switches has been observed with 200 ns voltage pulses.[27] This time duration is too small for any significant heating. Moreover, a simple application of the electrostatic image method demonstrates that charged particles immersed in the high dielectric water medium cannot penetrate any naturally occurring microbubbles due to the inherent electrostatic Coulomb repulsion. Hence, a separate mechanism, differing from the traditional viewpoint, has to be considered for the initiation of breakdown in liquids by short, nanosecond pulses.

Here we argue that strong field enhancement at the liquid-metal interface, caused by changes in liquid polarizability, is an important universal mechanism that could be a source of electronic breakdown at high applied voltages. The presence of large electric fields at the liquid-metal interface should produce a realignment of the strongly polar water molecules due to electrostatic interactions. Energy minimization would then lead to the formation of an ordered molecular lattice over a few molecular monolayers of the interface. As is well known, dipolar ordering reduces the effective polarization.[28,29] This reduction should, therefore, work to further strengthen the electric field based on considerations of local continuity for the electric displacement vector. A potential positive feedback mechanism can thus be initiated near the electrodes under high-voltage stress.

There is indeed some experimental justification for such

interesting high electric-field effects in water, based on recent reports in the chemical physics literature. For example, x-ray reflectivity measurements[30,31] have revealed that water density can be highly inhomogeneous, with the value at the electrodes being almost twice that of the bulk. This high density of water near the electrode surface has been postulated to result from electrostriction.[32] Similarly, phase transitions into a "solid water layer" close to the electrodes have been reported at high electric fields.[33,34] These collective experimental observations seem to suggest the following plausible scenario.

(i) Very high electric fields are capable of producing phase transitions and density variations in water. Since the fields are expected to be largest at electrodes and in the vicinity of the electrical double layer, tangible effects would be initiated and become observable at the contacts.
(ii) The density and permittivity variations could lead to local opaque regions (due to refractive index variations), as have been reported in water breakdown experiments.[27,35]
(iii) The induced changes in dipole moments could produce strong ponderomotive forces.[36,37] In order to balance the ponderomotive forces, atomic displacements would then lead to internal stress and electrostrictive density variations. Pressure buildup is a natural consequence and could become manifested as a shock wave. Such shock waves have indeed been observed in high-voltage, water-filled systems.[38–41]

In this contribution, we analyze the electrical double layer at the electrode-water interface for high-voltage devices close to the breakdown point, based on a Monte Carlo approach. This allows for the inclusion of field-dependent permittivity, and provides a self-consistent spatial distribution of the dipole structure, orientation, ionic concentrations and potentials. Dipole realignment effects, ion-ion correlation, finite-size effects, and other enhancements to the traditional Gouy-Chapman theory[42,43] are all comprehensively included. Our results show that strong increases in the surface electric fields with concomitant lowering of the dielectric constant could lead to dramatic enhancements in Schottky injection at the contacts. This process could be a source for initiating electronic controlled breakdown and provide for carrier multiplication through impact ionization close to the metal surfaces. The possibility for charge creation through electron initiated inelastic collisions in water has recently been demonstrated.[44,45] The Monte Carlo based calculations presented here also show that large pressures associated with the Maxwell stress tensor would be created at the electrode boundaries. Our results are shown to depend on the ionic density, in keeping with recent observations. A simple, perturbative analysis shows that high field regions with a sharp variation in permittivity can potentially be critical spots for instability initiation.

II. THE LIQUID-METAL INTERFACE

Before getting into the numerical details and results, it is perhaps helpful to briefly review the metal-liquid interface physics. This will also facilitate a quick comparative discussion of the various approaches used. The distribution of electrostatic potential at the metal electrode-liquid interface, usually referred to as the "electrical double-layer problem," has been the subject of electrochemical research for several decades. The classical theory of Gouy[42] and Chapman,[43] which appeared a decade before the Debye theory of bulk electrolytes,[46] is still the basis of research in this area. This is a mean-field theory based on the Poisson-Boltzmann equations, in which an equi-potential metallic surface is taken to be in contact with the solvent, regarded as a dielectric continuum. In this "primitive model," solvent structure is completely ignored. This theory also takes no account of ion size, and is thus unable to model charge saturation in the neighborhood of a blocking contact. It is also a poor approximation in the neighborhood of an ion, or near electrodes where the high local electric fields can modify the characteristic macroscopic properties. A significant modification, due to Stern,[47] suggested the use of a thin layer adjacent to the metal with dielectric properties different from the bulk from which all ions were excluded. In a sense, this was an attempt to describe changes in dielectric properties near the metal surface due to electrostatic interactions. Subsequent model advances included a position- and field-dependent dielectric constant for the Stern layer.

Many modern treatments of the double layer have made use of statistical approaches based on a homogeneous dielectric model with finite-size effects.[48,49] These approaches make use of either the Poisson-Boltzmann approach, the hypernetted chain approximation,[50,51] or the Ornstein-Zernike equation.[52,53] However, these schemes are quite complicated and are not really applicable to either medium-to-high ion densities or for double-layer potentials significantly larger than the thermal voltage. They also ignore the dynamical aspects. Another general drawback of such mean-field theories is that they ignore ion-correlation effects, which could become important at high ion concentrations. In order to overcome the deficiencies, several numerical methods have been proposed.[54–59] In the lattice-gas approach, a structured-layered model of ions and dipoles is used to include the finite-size effects and field-dependent dielectric saturation based on Langevin behavior.[59] The primary drawback is the inability to incorporate local lattice disorder, arising from thermal fluctuations and/or multi-impurity species.

The most reliable and accurate methods for modeling the double-layer problem at the electrode-liquid interface have been through the kinetic, hard-sphere approaches based on computer-intensive Monte Carlo and molecular dynamics schemes.[54–58] In these schemes, both the ions and the solvent are treated on an equal footing, in terms of discrete, finite-size particles. These numerical models capture many important features, such as the highly organized layering of ions near a metallic surface and the possibility of charge inversion. Treating the polar solvent as dipoles allows the self-consistent incorporation of the solvent structure into the double layer. The effects of steric repulsion can also be included.[60] Though hydrophobic and hydrophilic interaction have not yet been treated, it seems possible to incorporate these aspects through the use of Lennard-Jones potentials

with finite cutoffs as done in the biophysics area.[61] Moreover, such kinetic approaches are simple to implement, easily provide for a three-dimensional analysis, and can accommodate irregular boundaries. Given the accuracy, transparency, and ease of numerical implementation, the Monte Carlo scheme will be used in the present analysis of the metal-liquid interface at high externally applied voltages.

III. MODELING DETAILS

The primary aim here is to analyze the static properties of the electric double layer at the metal-water interface in the presence of large externally applied voltages. Details of the transient development in response to an externally applied voltage are beyond the present scope. Hence, the static, canonical Monte Carlo approach[62–65] was chosen here, instead of the dynamic molecular dynamics simulation method.[28] The ions (for a given user specified average density) were modeled as charged Lennard-Jones (LJ) spherical particles. Here, Na^+ and Cl^- ions were considered. Water molecules were treated in terms of the rigid SPC/E model, which consists of three partial charges located on the oxygen and hydrogen sites.[66] Unlike most previous reports, the dipole-ion and dipole-dipole interactions were explicitly included in our calculations, in addition to the usual many-body, ion-ion interactions. The LJ parameters for the ion-ion and ion-water interactions were taken from reports in the literature.[67,68] The interaction of the electrolyte solution with the metal electrode was assumed to consist of a nonelectrostatic, due to the externally applied electric field, and an electrostatic image charge contribution. Surface corrugation effects and interactions between metal-oxygen and metal-hydrogen, as described by Spohr,[69] were incorporated into the simulation model. The corrugation attempts to describe the surface inhomogeneity due to the discrete location of atomic cores. In this scheme, the metal-oxygen interaction is described by a Morse function, augmented by a corrugation term. The metal-hydrogen interaction is modeled by an exponentially repulsive potential.[69] The corrugation is felt only in the repulsive part of the Morse potential function, and was taken to have a periodicity of 3.6 Å in both directions parallel to the surface. The metallic nature of the electrode (perfect conductor) was modeled by the image charge method, with the image plane located at the $z=0$ boundary, and the solution lying in the $z>0$ region. Each charge q_j in the system, whether a partial charge of the water molecule or an ionic charge, was taken to interact with all other real charges and also the image charges $q_j^I(=-q_j)$.

The simulation volume ($z>0$) consisted of a mixture of N_+ cations with charge q_+ of particle diameter d_+ and N_e anions of charge q_- with particle diameter d_-, in addition to N_μ dipoles of moment μ and diamater d_μ. The SPC/E model was used to assign partial charges to each water dipole cluster. The particles were confined in a rectangular simulation cell with dimensions of $W\times W\times L$. Hard walls were assumed along the boundaries normal to the z axis, and periodic boundary conditions were applied along the lateral directions. The potential energy of the system was obtained by a pairwise summation of all the two-particle interactions and the one-particle energies in the externally applied field. Long-range corrections for the Coulomb interactions were taken into account by a tabulated version of the Ewald sum for a slab system with infinite extent along the two transverse directions.[70] The pair interactions acting between the various species of molecules are the well-known multipole potentials with the corresponding hard sphere (HS) repulsive cores. The HS core potential $U_{HS}(r_{ij},d)$ usually had the form $U_{HS}(r_{ij},d)=\infty$ for $r_{ij}<d$, and $U_{HS}(r_{ij},d)=0$ otherwise. The two-particle energies for the ion-ion (U_{ii}), the ion-dipole ($U_{i\mu}$), and the dipole-dipole ($U_{\mu\mu}$) terms were taken from the work of Boda, Chan, and Henderson.[71] In the overall process, many-body interactions and screening are naturally taken into account.

For the Monte Carlo simulations, the initial configuration was set up by placing the N_+ cations, the N_- anions, and N_μ water molecules randomly within the simulation volume. A random orientation of the hydrogen atoms with respect to the oxygen was assigned as the initial starting condition for all the water molecules. This yielded the total initial energy of the system. Subsequently, at each step, a randomly chosen particle was moved to a new location within the simulation box. This move was accepted only if it decreased the resulting energy of the system. As a result, the system configuration was made to evolve towards a lower energy state through such random assignments, and it resembles a Markov process that allows fluctuations in the local density. For moves involving a water molecule, the position of the oxygen atom was randomly chosen. Of the six remaining coordinates for the two hydrogen atoms, three were assigned randomly, while the remaining three were deterministic in keeping with the H-O bond lengths and the H-O-H bond angle. These configurational jumps were repeatedly well over a million times to evolve the system towards a stable, final-state configuration. The simulations were carried out for a constant global density of 10^3 Kg m^{-3}, and so no additions or deletion of particles was permitted. Information relating to the dipole moments and local electric fields could be calculated as a function of position for each configuration. Values of the dipole moment yielded the relative permittivity ε_r based on the second central moment, as given by the following relation:[72,73]

$$\varepsilon_r = 1 + \frac{4\pi}{3}\frac{\langle M^2\rangle - \langle M\rangle^2}{\varepsilon_0 V k_B T}, \tag{1}$$

where $\langle M\rangle$ is the mean dipole moment of the water molecules, ε_0 the free-space permittivity, V the volume, k_B the Boltzmann constant, and T the temperature in kelvin.

IV. RESULTS AND DISCUSSION

The Monte Carlo (MC) scheme was applied to analyze the electric double layer at the electrode-water interface with consideration of both the ions and water dipoles. Results are first presented for pure water without any ions for simple model validation. Figure 1 shows the radial distribution function (RDF) between oxygen atoms, $g_{oo}(r)$, obtained from the present MC simulations. The RDF represents the probability of finding a second particle at a separation r from the first,

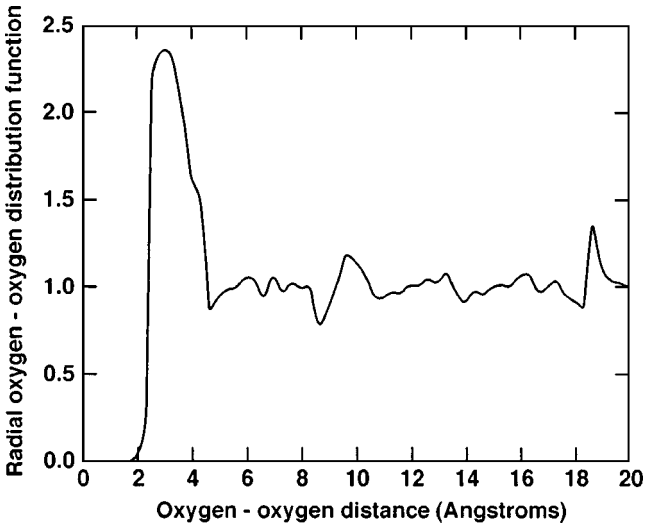

FIG. 1. Simulation results showing the radial distribution function $g_{oo}(r)$ for pure water.

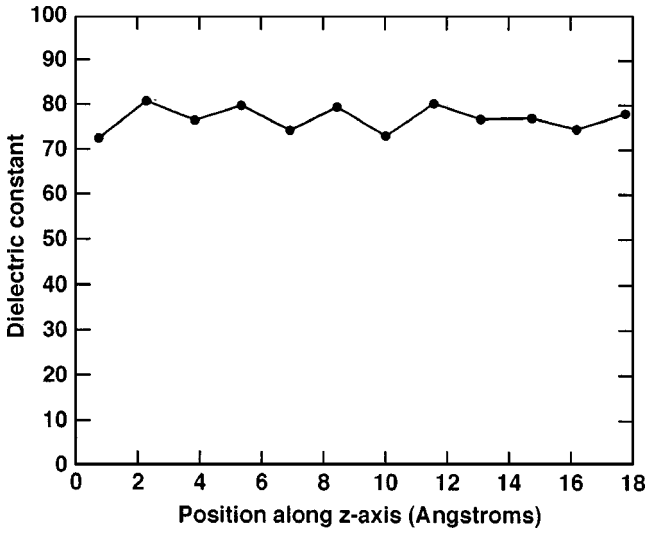

FIG. 3. The spatial variation, obtained from the MC in a direction (z axis) normal to the metal electrodes for pure water without an external field.

and so provides information on the local structure of a molecular system. Our result for $g_{oo}(r)$ matches previous experimental reports obtained from neutron diffraction and x-ray scattering measurements,[74,75] and is also in keeping with other calculations.[76] The hydrogen-hydrogen and hydrogen-oxygen RDFs (not shown) were also in good agreement with published reports. Results of the dielectric function for pure water in the absence of any ions or impurities, or external electrode potential, from the dipole moments [as given in Eq. (1)], are shown in Fig. 2. The values were obtained as a function of the MC simulation steps. The overall magnitude is seen to fluctuate in a range close to the accepted value of ~80 for water and stabilizes at about 77.01 after 30 million Monte Carlo steps. The curve of Fig. 2 represents the global average for the entire simulation region. The spatial variation, obtained from the MC code, is shown in Fig. 3 along a direction (z axis) normal to the metal electrodes. An average over the last 1000 time steps was used for smoothening the data of Fig. 3. The main feature, once again, is the nearly uniform value of about 77.01 with some fluctuating behavior.

The field dependence of the dielectric function was next probed by running the MC simulations for pure water, but with a uniform potential at the electrodes. A negative charge density of 0.5 C m^{-2} was assigned at the left wall (the cathode), taken to lie in the $z=0$ plane. Due to the presence of this high electric field at the surface, strong orientation of the water dipoles can be expected that should lead to a decrease in the value of the dielectric function. Results of ε_r from the simulation close (within 20 Å) to the electrode surface are shown in Fig. 4 as a function of the MC steps. A final value of roughly 5.0 is obtained, and is indicative of the strong alignment effect produced by the electric field that significantly lowers the local permittivity. As might be expected, the molecular orientation effect is the strongest near the electrode boundary (at $z=0$) and gradually weakens with distance. Figure 5, which shows the spatial dependence of the

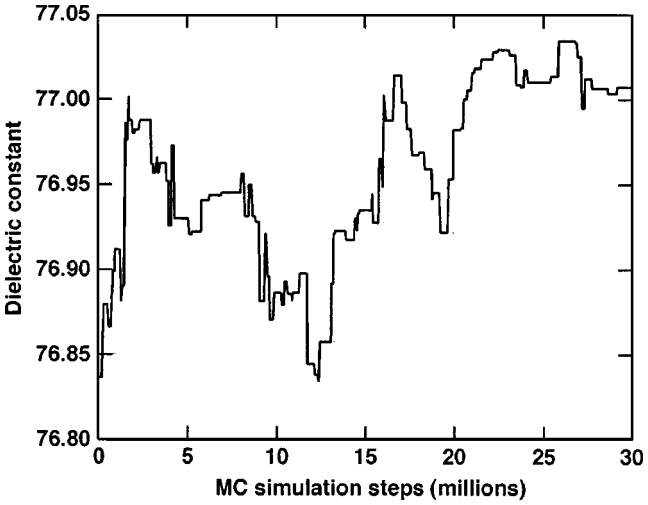

FIG. 2. Calculations of the global average of the dielectric function for pure water in the absence of any ions or impurities, or external electrode potential, as a function of the simulation steps.

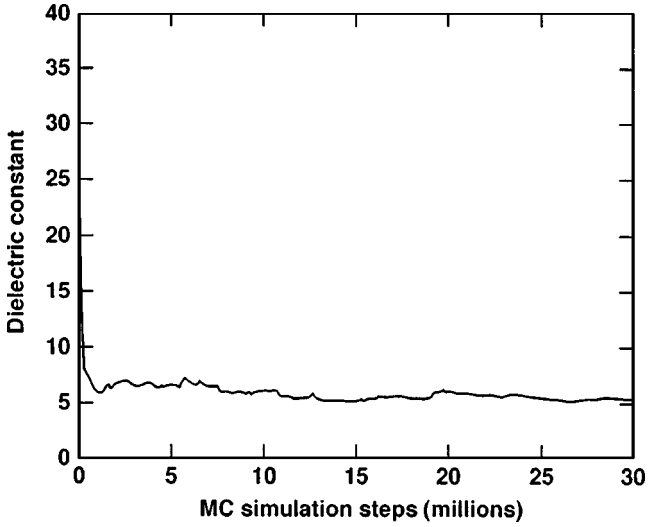

FIG. 4. Calculations of the relative permittivity close to the electrode (within 20 Å) as a function of the MC steps for pure water. A charge density of 0.5 C m^{-2} was assigned to the left wall at $z=0$.

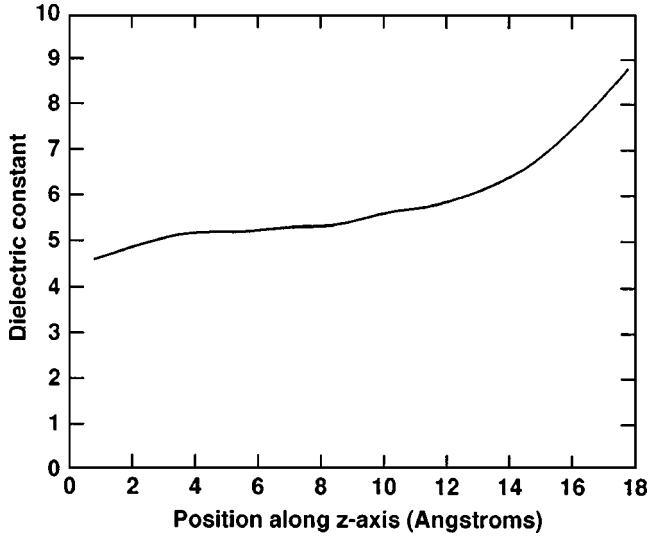

FIG. 5. The spatial dependence of the dielectric function for the case of Fig. 4.

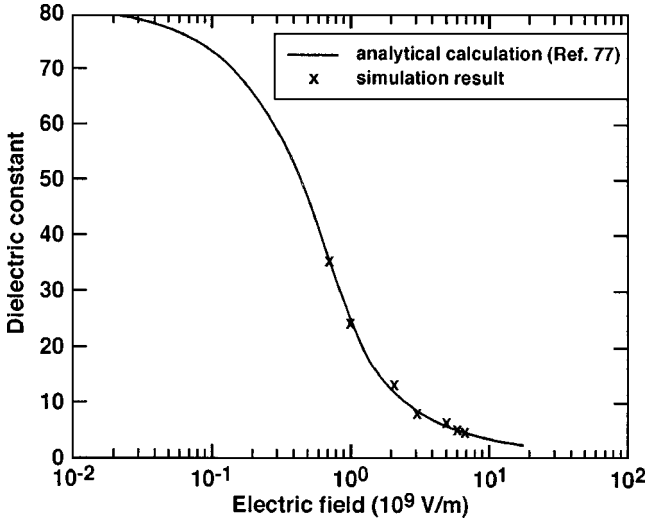

FIG. 7. Data points for the field dependent relative permittivity obtained from the current Monte Carlo and a theoretical curve of Ref. 77.

dielectric function, provides a quantitative picture. Within about 18 Å, the value is predicted to roughly double, starting from about 5 at the electrode interface. Such a transition from a very ordered layer near the surface to a more disoriented region farther from the electrode surface had been predicted by lattice models.[59] This dipole ordering and its spatial dependence normal to the electrode surface are better reflected in the angular distribution of Fig. 6. The dipole angle θ, with respect to the z axis, is a variable between 0 and π. Due to dipole orientation, the values of θ are closer to π as seen in Fig. 6, with a gradual trend towards randomization with increasing distance z from the metal surface.

Based on position-dependent evaluations of both the electric field (E) and relative permittivity from the MC simulations, the relation between ε_r and E was next obtained. Varying the initial charge density on the metallic electrode allowed for changes in the peak electric field. Monte Carlo data for the relative permittivity thus obtained are shown in Fig. 7, along with a recent theoretical prediction.[77] The MC calculations were limited to a finite electric-field range due to the computational burden. In any case, Fig. 7 reveals very good agreement with a previous analytical calculation and clearly demonstrates the monotonically decreasing trend in permittivity with electric field. Position-dependent data (along the z axis) for both the electric field and permittivity were then used for calculations of the internal pressure based on the Maxwell stress tensor. The internal pressure due to the electric field stress as a function of position is shown in Fig. 8. Combining the pressure $P(z)$ along the z distance with the electric-field variation along z yielded the pressure versus electric-field curve. This is indirectly indicative of the electrostrictive effect at high electric fields in water. Figure 9 shows the simulation data for electric fields in the range from 2×10^9 to 6.5×10^9 V m^{-1}. A recent analytical prediction[77] is also shown for comparison. The figure demonstrates that very large pressures on the order of GPa can be created at the high electric fields. Under uniform, equilibrium conditions, atomic forces that arise due to perturbations in the local den-

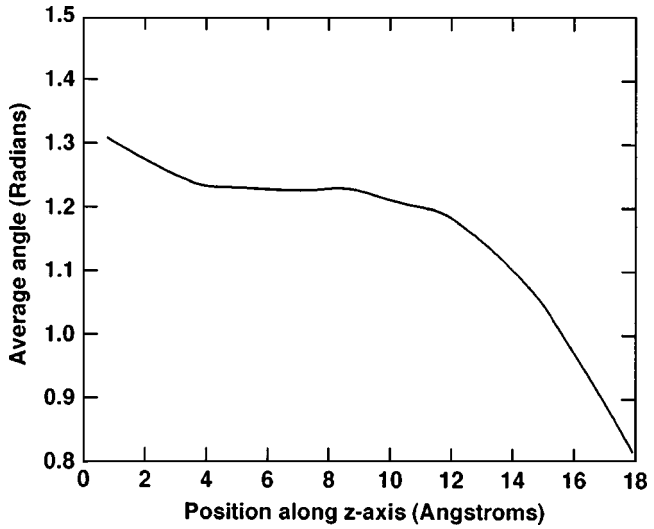

FIG. 6. The corresponding angular distribution of the water dipoles as a function of the normal distance.

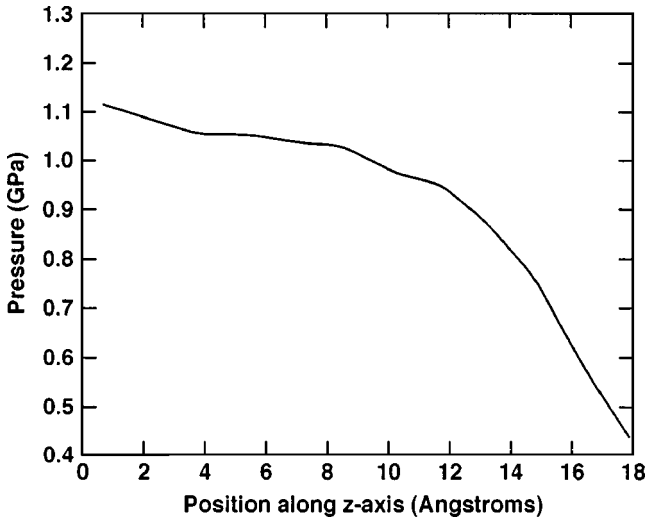

FIG. 8. Internal pressure due to the applied potential as a function of the z distance. A charge density of 0.5 C m^{-2} was assumed at the $z=0$ electrode.

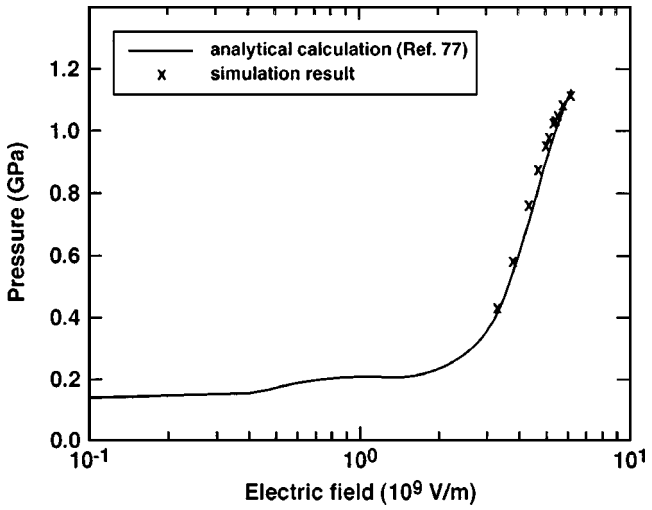

FIG. 9. Data points for the pressure vs electric field obtained from the Monte Carlo simulations and a theoretical curve from Ref. 77.

sity will balance the electrostatic stress. For a more general case of spatial nonuniformity, however, as might result from the discrete positioning of finite-sized ions, or corrugations at the metallic surface, large lateral stress can also be created. Dynamic motion of ions could result in potential instabilities and shock waves as have been observed experimentally.[38–41]

Having discussed the role of the electric field on the polarizability and dipole orientation in pure water, simulation results that include Na^+ and Cl^- ions are presented next. Three ion pairs were used for a 18 Å cubical simulation box. As previously stated, the initial condition for all water molecules consisted of a random orientation of the two hydrogen atoms at a fixed distance from each oxygen site. The *z*-dependent dielectric constant, near the negative electrode, obtained from MC simulations, is shown in Fig. 10. A quick comparison between the previous calculation for pure water (shown in Fig. 5) and the present result reveals two very important features.

(i) First, a fairly pronounced local maxima in ε_r is evident near the 4 Å point. Physically, this behavior can be understood in terms of the field perturbation caused by the Na^+ ions. The region close to the electrode surface has a random distribution of Na^+ ions, each with a finite radius of about 1.9 Å. The first layer of ions is, on an average, at a distance of about 2 Å from $z=0$. Due to the interatomic, core repulsion, the next set of ions is separated by roughly 4 Å. Thus, near the $z\sim 4$ Å plane lies approximately midway between two adjacent sheets of ions and has a lowest resulting electric field. Consequently, the magnitude of ε_r is predicted to be the highest at around this location. At large distances (i.e., $z>12$ Å) the density of ions is no longer as high, and so the ionic perturbative effects to the overall electric field distribution become less pronounced. A gradual, monotonic increase in ε_r is predicted, as orientational effects on the water dipoles get weaker. In any event, a definite spatial structure in the local permittivity is predicted. This is in contrast to the usual assumptions of either uniform or monotonic distributions. Such local fluctuations imply that the refractive index and hence the optical properties should also have possible striations. This is qualitatively similar to recent high-voltage experiments on water by our group, which have shown localized opaque regions near electrodes based on Schlieren techniques.[27] The length scales here, however, are much smaller. An interesting feature of Fig. 10 is that the slope $d\varepsilon_r/dz$ can take on both negative and positive values depending on the location. As will be shown, this can potentially lead to instabilities that originate near the electrode.

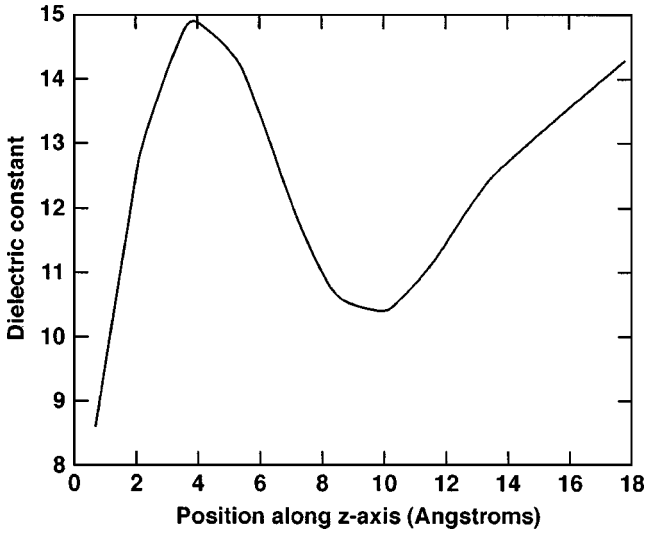

FIG. 10. Spatial dependence of the dielectric function with Na^+ ions in water.

(ii) A second feature of Fig. 10, relative to the previous curve of Fig. 5, is the much higher value of ε_r near the $z=0$ electrode surface. This again arises from the perturbative effects of the ions near the boundary. Strong Coulomb forces produced by the ions disturb the near-perfect orientation of water dipoles that could be set up by the external field. Consequently, the average dipole moment $\langle M\rangle$ is not quite as large, and based on Eq. (1), the resulting permittivity is not as small. Obviously, variations in the ion density can be expected to influence the degree of perturbation. As a result, magnitudes of the surface fields, permittivity, and eventually the breakdown strength can all be expected to be density dependent. Such an ion-density dependence of the breakdown voltage has recently been observed by our group. Finally, calculations of internal pressure for the water-ion system are shown in Fig. 11. The nonuniformity is once again evident, and can, in principle, lead to a locally triggered instability.

A couple of final comments relating to the results presented are perhaps in order. First, the dramatic lowering of the permittivity at the electrode surfaces implies that a natural mechanism for electric-field enhancement exists irrespective of possible contributions from electrode roughness. The electron injection current I_{SE} at the cathode due to the Schottky-emission process is $\sim K_0 \exp[K_1 (E/\varepsilon_r)^{1/2}]$, where

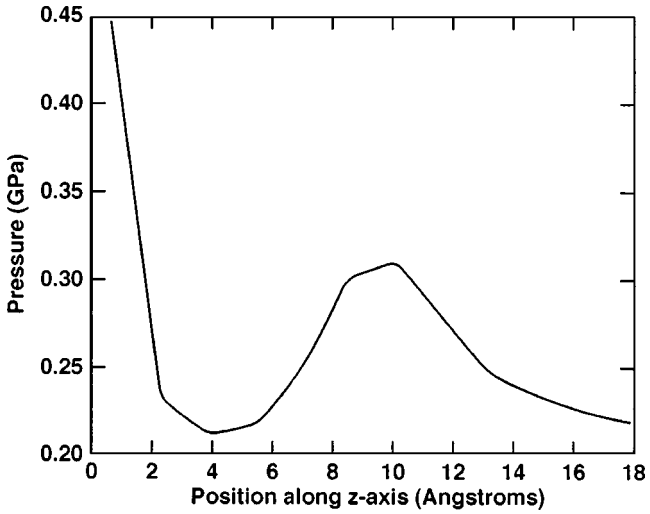

FIG. 11. Results for the internal pressure with normal distance from the negative electrode for water containing Na^+ ions.

E is the electric field and $K_{0,1}$ are field-independent constants. Consequently, an increase in E with a corresponding reduction in ε_r can potentially provide large enhancements in the Schottky injection current. Since such injection can trigger breakdown, this poses a fundamental limit on the maximum voltage that can be applied.

Finally, we turn to the instability issue and show that the above results support the possibility of uncontrolled charge growth near an electrode. For concreteness, we focus on the cathode, which is taken to be at the $z=0$ surface. A one-dimensional analysis is used to probe time-dependent, perturbative effects of a negative charge fluctuation, as might arise from electron injection. The local electric field $E(z,t)$ and ion density $N^-(z,t)$ can be expressed in terms of a static and a small-signal time varying component as

$$E(z,t) = E_0(z) + E_1 \exp[j(kz - \omega t)], \tag{2a}$$

$$N^-(z,t) = N_0^-(z) + N_1^- \exp[j(kz - \omega t)], \tag{2b}$$

where $N_0^-(z)$ and $E_0(z)$ are the static distributions of the negative ion density and electric field, respectively, ω is the angular frequency of a possible disturbance, k the corresponding wave number, and E_1 and N_1 are the magnitudes of dynamic perturbations in electric field and number density. In the above, $E_0(z)$ is negative in value due to the assumed cathode location at $z=0$. Fluctuations in the electric field will produce corresponding dynamic variations in the relative permittivity, and these can be expressed as

$$\varepsilon_r[E(z,t)] = \varepsilon_r\{|E_0(z)|\} + \{d[\varepsilon_r(E)]/dE\}E_1 \exp\{j(kz - \omega t)\}. \tag{3a}$$

In Eq. (3a), the value of $d[\varepsilon_r(E)]/dE$ is negative due to the monotonic decrease in ε_r with increasing electric field. Using the notation $K=-d[\varepsilon_r(E)]/dE$ for compactness, the expression for the displacement vector $D=\varepsilon_0\,\varepsilon_r\,E$ is then given as

$$D(z,t) = \varepsilon_0\,[\varepsilon_r\{|E_0(z)|\} - KE_1 \exp\{j(kz - \omega t)\}][E_0(z) + E_1 \exp\{j(kz - \omega t)\}]. \tag{3b}$$

Ignoring higher order terms in the perturbation, $D(z,t)$ becomes

$$D(z,t) \sim \varepsilon_0\varepsilon_r\{|E_0(z)|\}E_0(z) + \varepsilon_0 E_1 \exp\{j(kz - \omega t)\} \times[\varepsilon_r\{|E_0(z)|\}] - KE_0(z)]. \tag{3c}$$

The usual Poisson equation and the constitutive relation for current density J are

$$dD(z,t)/dz = q[N_0^+(z) - N^-(z,t)], \tag{4a}$$

$$J \sim qE(z,t)[N_0^+(z)\mu^+ + N^-(z,t)\mu^-] + dD(z,t)/dt, \tag{4b}$$

where the diffusion current component has been ignored. In Eq. (4b), μ^+ and μ^- are the positive and negative ion mobilities, respectively. Using expressions for $D(z,t)$ from Eq. (3c) and for $N^-(z,t)$ from Eq. (2b) in Eq. (4a), and retaining only first-order time-dependent terms lead to

$$qN_1 = \varepsilon_0\{KE_1 dE_0(z)/dz + ikKE_1E_0 - ik\varepsilon_r[|E_0(z)|]E_1\}. \tag{4c}$$

Finally, the first-order time-dependent terms of Eq. (4b) in conjunction with Eq. (4c) above, yield the following dispersion relation:

$$\omega = -k\mu^-E_0 - i[N_0^-q\mu^- + \mu^-E_0KdE_0(z)/dz]/ [\varepsilon_0\varepsilon_r[\{|E_0|\}] - \varepsilon_0KE_0]. \tag{4d}$$

Unstable behavior requires that the imaginary part of ω be positive. Since K is positive, while $E_0<0$, this implies the denominator of the imaginary term of Eq. (4d) will be positive. Hence, instability requires that the numerator $[N_0^-q\mu^- + \mu^-E_0KdE_0(z)/dz]<0$. Thus, instability for the liquid water stressed to high voltages can arise provided $dE_0(z)/dz$ is positive and exceeds $-qN_0^-/[KE_0]$ in magnitude. The most favorable conditions for instability then are at electric fields for which the product $KE_0=-E_0d[\varepsilon_r(E)]/dE$ is large and/or for low ion density N_0^-. For water, the decrease in permittivity with electric field is the largest at about 4.5 MV/cm (e.g., as in Ref. 77). This, therefore, represents a potentially critical operating point. It could signify a natural upper bound on electric field stressing for stable operation of water at a given bulk conductivity.

V. SUMMARY AND CONCLUSIONS

In conclusion, we have analyzed the electrical double layer at the electrode-water interface for high-voltage devices close to the breakdown point, based on a static, Monte Carlo approach. The primary goal was to attempt a better understanding of the inherent physics at the water-electrode interface, and its effects on high-voltage, electrical operation. The MC calculations carried out here attempt to address some of the open questions. These include the potential mechanism for breakdown initiation, assessing the fundamental limits on electric-field stressing, and the potential for instabilities and streamer generation. While these issues remain to be studied in detail, our results demonstrate the pos-

sibility of strongly nonlinear field-induced effects near the electrodes. This is a particularly important region, since a variety of features such as the appearance of opaque optical areas, streamer initiation, shock-wave generation, and illuminated spots have all been observed at high applied voltages near the electrodes.

It has been shown that strong dipole realignment, ion-ion correlation, and finite-size effects can greatly modify the electric fields and local permittivity at the electrode interface. The sharp increase in the surface electric fields with concomitant lowering of the dielectric constant could lead to dramatic enhancements in Schottky injection at the contacts. This process could, therefore, be a source for initiating electronic controlled breakdown and provide for carrier multiplication through impact ionization close to the metal surfaces. Due to electrode corrugation, as well as the finite-size effects of ions and molecules, a transverse dependence on the Schottky enhancement should exist. This would then be responsible for localized charge creation and streamer growth and propagation.

The Monte Carlo based calculations presented here also showed that large pressures associated with the Maxwell stress tensor would be created at the electrode boundaries. The pressure dependence on the electric field obtained here matched a previous report that had been based on analytical, thermodynamic calculations.[77] It was demonstrated that the enhancement would depend on the background conductivity of liquid water, and is in keeping with observations of breakdown voltages that depend on bulk conductivity. The MC results also demonstrated that the Coulomb forces due to ions near the interface modify the dipole arrangement to produce local structure and striations in local permittivity. Though the lateral structure was not studied, it is implicit that some degree of transverse variations is also to be expected.

A simple, perturbative analysis was carried out to probe the potential instability at the electrodes. It was shown that a high field region with the steepest slope for $d[\varepsilon_r(E)]/dE$ can potentially be a critical spot for instability initiation. In order to avoid such instabilities and extend the operating voltages, one would need to reduce the possibility of charge injection, or using liquids with an inherently lower $d[\varepsilon_r(E)]/dE$ slope. The former would require the utilization of smooth electrode surfaces through careful polishing, and/or the use of composite materials with large barrier heights at the cathodes. Since electron injection is not an ongoing mechanism at the anode (perhaps it would be field ionization instead), an optimized design *might require the use of two different electrode materials.* Finally, nonpolar liquids might also help increase the high-voltage operation by naturally lowering the $|d[\varepsilon_r(E)]/dE|$ magnitude. For example, reports on the breakdown strength for oils indicate a maximum value of about 4 MV/cm,[78] while the highest reports for water are close to 2 MV/cm.[27]

ACKNOWLEDGMENTS

This work was sponsored by an AFOSR-MURI grant on Compact, Portable Pulsed Power. One of us (R.P.J.) appreciates useful discussions with J. Lehr (Sandia National Laboratory).

[1]H. Akiyama, IEEE Trans. Dielectr. Electr. Insul. **7**, 646 (2000).
[2]J. Talati, T. Shah, A. Memon, M. Sidhwa, S. Adil, and A. Omair, J. Urol. (Baltimore) **146**, 1482 (1991).
[3]A. H. Olson and S. P. Sutton, J. Acoust. Soc. Am. **94**, 2226 (1993).
[4]M. Zahn, Y. Ohki, D. B. Fenneman, R. J. Gripshover, and V. Gehman, Jr., Proc. IEEE **74**, 1182 (1986).
[5]M. R. Patel, M. A. Barrufet, P. T. Eubank, and D. D. DiBitonto, J. Appl. Phys. **66**, 4104 (1989).
[6]I. Vitkovitsky, *High Power Switching* (Van Nostrand Reinhold Company, New York, 1987), pp. 116–137.
[7]R. P. Joshi, J. Qian, and K. H. Schoenbach, J. Appl. Phys. **92**, 6245 (2002).
[8]P. K. Watson and A. H. Sharbaugh, J. Electrochem. Soc. **107**, 516 (1960).
[9]N. J. Felici, J. Electrost. **12**, 165 (1982); IEEE Trans. Electr. Insul. **20**, 233 (1985).
[10]A. Nikuradse, *Das Flüssige Dielektrikum* (Springer, Berlin, 1934), pp. 134–152.
[11]F. Pontiga and A. Castellanos, IEEE Trans. Dielectr. Electr. Insul. **3**, 792 (1996).
[12]E. E. Kunhardt, Phys. Rev. B **44**, 4235 (1991); H. M. Jones and E. E. Kunhardt, J. Appl. Phys. **77**, 795 (1995).
[13]E. O. Forster, IEEE Trans. Electr. Insul. **25**, 45 (1990).
[14]T. J. Lewis, IEEE Trans. Electr. Insul. **20**, 123 (1985).
[15]P. Keith Watson, W. G. Chadband, and M. Sadeghzadeh-Araghi, IEEE Trans. Electr. Insul. **26**, 543 (1991).
[16]A. Beroual, C. Marteau, and R. Tobazeon, IEEE Trans. Electr. Insul. **23**, 955 (1988); T. Aka-Ngnui and A. Beroual, J. Phys. D **34**, 794 (2001).
[17]J. Qian, R. P. Joshi, K. H. Schoenbach, E. Schamiloglu, and C. Christodoulou, IEEE Trans. Plasma Sci. **30**, 1931 (2002).
[18]M. Carmo Lanca, J. N. Marat-Mendes, and L. A. Dissado, IEEE Trans. Dielectr. Electr. Insul. **8**, 838 (2001).
[19]E. O. Forster, IEEE Trans. Electr. Insul. **20**, 891 (1985).
[20]R. E. Hebner, J. Phys. D **35**, 205 (2002).
[21]P E Frayssines, N Bonifaci, A Denat, and O Lesaint, J. Phys. D **35**, 369 (2002).
[22]L. Niemeyer, L. Pietronero, and H. J. Wiesmann, Phys. Rev. Lett. **52**, 1033 (1984).
[23]P. P. Wong and E. O. Forster, IEEE Trans. Electr. Insul. (to be published).
[24]I. V. Lisitsyn, H. Nomiyama, S. Katsuki, and H. Akiyama, IEEE Trans. Dielectr. Electr. Insul. **6**, 351 (1999).
[25]M. Szklarczyk, *Modern Aspects of Electrochemistry*, edited by J. O'M Bockris, B. E. Conway, and R. E. White (Plenum, New York, 1993), 25, pp. 253–296.
[26]J. V. Coe, A. Earhart, M. H. Cohen, G. J. Hoffman, H. W. Sarkas, and K. H. Bowen, J. Chem. Phys. **107**, 6023 (1997).
[27]S. Xiao, J. Kolb, S. Kono, S. Katsuki, R. P. Joshi, M. Laroussi, and K. H. Schoenbach, IEEE Trans. Dielectr. Electr. Insulation (to be published).
[28]I. C. Yeh and M. L. Berkowitz, J. Chem. Phys. **110**, 7935 (1999).
[29]A. Kornyshev and G. Sutmann, J. Electroanal. Chem. **450**, 289 (1998).
[30]M. F. Toney, J. N. Howard, J. Richer, G. L. Borges, J. G. Gordon, O. R. Melroy, D. G. Wiesler, D. Yee, and L. B. Sorensen, Nature (London) **368**, 444 (1994).
[31]M. F. Toney, J. N. Howard, J. Richer, G. L. Borges, J. G. Gordon, O. R. Melroy, D. G. Wiesler, D. Yee, and L. B. Sorensen, Surf. Sci. **335**, 326 (1995).
[32]I. Danielewicz-Ferchmin and A. R. Ferchmin, J. Phys. Chem. **100**, 17281 (1996).
[33]J. J. Kasinski, L. A. Gomez-Jahn, K. J. Faran, S. M. Gracewski, and R. J. Dwayne Miller, J. Phys. Chem. **90**, 1253 (1989).
[34]Y. S. Chu, T. E. Lister, W. G. Cullen, H. You, and Z. Nagy, Phys. Rev. Lett. **86**, 3364 (2001).
[35]E. V. Yanshin, I. T. Ovchinnikov, and Y. N. Vershinin, Sov. Phys. Tech. Phys. **18**, 1303 (1974).
[36]H. W. Jackson, Phys. Rev. B **25**, 3127 (1982).
[37]L. D. Landau and E. M. Lifshitz, *Electrodynamics of Continuous Media* (Pergamon, New York, 1960), Sec. 15.

[38]R. Pecha and B. Gompf, Phys. Rev. Lett. **84**, 1328 (2000).
[39]J. B. Homer and I. R. Hurle, Proc. R. Soc. London, Ser. A **314**, 585 (1969).
[40]F. Jomni, F. Aitken, and A. Denat, J. Acoust. Soc. Am. **107**, 1203 (2000).
[41]S. Madhavan, P. M. Doiphode, and S. Chaturvedi, IEEE Trans. Plasma Sci. **28**, 1552 (2000).
[42]G. Gouy, J. Phys. (Paris) **9**, 457 (1910).
[43]D. L. Chapman, Philos. Mag. **25**, 475 (1913).
[44]C. Champion, Phys. Med. Biol. **48**, 2147 (2003); C. Champion, J. Hanssen, and P. A. Hervieux, J. Chem. Phys. **117**, 197 (2002).
[45]S. Uehara, H. Nikjoo, D. T. Goodhead, and T. C. Dudley, Radiat. Res. **152**, 202 (1999); S. Uehara, H. Nikjoo, and G. T. Goodhead, Phys. Med. Biol. **38**, 1841 (1993).
[46]P. Debye and W. Huckel, Phys. Z. **24**, 185 (1924); **24**, 305 (1924); **25**, 97 (1924).
[47]O. Stern, Z. Elektrochem. **30**, 508 (1924).
[48]D. Henderson and L. Blum, Surf. Sci. **101**, 189 (1980).
[49]C. W. Outhwaite, L. B. Bhuiyan, and S. Levine, J. Chem. Soc., Faraday Trans. 2 **76**, 1388 (1980).
[50]G. M. Torrie, P. G. Kusalik, and G. N. Patey, J. Chem. Phys. **88**, 7826 (1988).
[51]G. M. Torrie and G. N. Patey, Electrochim. Acta **36**, 1669 (1991).
[52]D. Henderson, F. Abraham, and J. Barker, Mol. Phys. **100**, 129 (2002).
[53]M. Yasutomi, J. Phys.: Condens. Matter **13**, L255 (2001).
[54]G. M. Torrie and J. P. Valleau, J. Chem. Phys. **73**, 5807 (1980).
[55]D. M. Heyes, Chem. Phys. **69**, 155 (1982).
[56]S. H. Suh, L. M. Teran, H. S. White, and H. T. Davis, Chem. Phys. **142**, 203 (1990).
[57]R. Guidelli, G. Aloisi, M. Carlá, and M. R. Moncelli, J. Electroanal. Chem. **197**, 143 (1986).
[58]L. Zhang, H. T. Davis, and H. S. White, J. Chem. Phys. **98**, 5793 (1993).
[59]J. R. MacDonald, Surf. Sci. **116**, 135 (1982); J. R. MacDonald and S. H. Liu, *ibid.* **125**, 653 (1983).
[60]V. Russier, J. P. Badiali, and M. L. Rosinberg, J. Electroanal. Chem. **220**, 213 (1987).
[61]O. Farago, J. Chem. Phys. **119**, 595 (2003).
[62]H. Greberg, R. Kjellander, and T. Akesson, Mol. Phys. **92**, 35 (1997).
[63]B. Svensson, B. Jonsson, and W. E. Woodward, Biophys. Chem. **38**, 179 (1990).
[64]I. Ruff, A. Baranyai, G. Palinkas, and K. Heinzinger, J. Chem. Phys. **85**, 2169 (1986).
[65]S. L. Carnie and D. Y. C. Chan, J. Phys. Chem. **73**, 2949 (1980).
[66]H. J. C. Berendsen, J. R. Grigera, and T. P. Straatsma, J. Phys. Chem. **91**, 6269 (1987).
[67]D. E. Smith and L. X. Dang, J. Chem. Phys. **100**, 3757 (1994).
[68]S. H. Lee, J. Chem. Phys. **101**, 6964 (1994).
[69]E. Spohr, J. Mol. Liq. **64**, 91 (1995).
[70]Y. J. Rhee, J. W. Halley, J. Hautman, and A. Rahman, Phys. Rev. B **40**, 36 (1989).
[71]D. Boda, K. Y. Chan, and D. Henderson, J. Chem. Phys. **109**, 7362 (1998).
[72]M. Neuann, Chem. Phys. Lett. **95**, 417 (1983).
[73]J. Anderson, J. Ullo, and S. Yip, Chem. Phys. Lett. **152**, 447 (1988).
[74]A. K. Soper, Chem. Phys. **258**, 121 (2000).
[75]G. Hura, J. M. Sorenson, R. M. Glaeser, and T. Head-Gordon, J. Chem. Phys. **113**, 9140 (2000); J. M. Sorenson, G. Hura, R. M. Glaeser, and T. Head-Gordon, *ibid.* **113**, 9149 (2000).
[76]P. G. Kusalik and I. M. Svishchev, Science **265**, 1219 (1994).
[77]I. Danielewicz-Ferchmin and A. R. Ferchmin, Chem. Phys. Lett. **351**, 397 (2002).
[78]A. Neuber (private communication).